Letter

^{1}H Hyperpolarization of Solutions by Overhauser Dynamic Nuclear Polarization with ^{13}C−^{1}H Polarization Transfer

Yu Rao, Amrit Venkatesh, Pinelopi Moutzouri, and Lyndon Emsley*

Read Online

ACCESS | 📊 Metrics & More | 📖 Article Recommendations | 🔵 Supporting Information

ABSTRACT: Dynamic nuclear polarization (DNP) is a method that can significantly increase the sensitivity of nuclear magnetic resonance. The only effective DNP mechanism for *in situ* hyperpolarization in solution is Overhauser DNP, which is inefficient for ^{1}H at high magnetic fields. Here we demonstrate the possibility of generating significant ^{1}H hyperpolarization in solution at room temperature. To counter the poor direct ^{1}H Overhauser DNP, we implement steady-state ^{13}C Overhauser DNP in solutions and then transfer the ^{13}C hyperpolarization to ^{1}H via a reverse insensitive nuclei enhanced by polarization transfer scheme. We demonstrate this approach using a 400 MHz gyrotron-equipped 3.2 mm magic angle spinning DNP system to obtain ^{1}H DNP enhancement factors of 48, 8, and 6 for chloroform, tetrachloroethane, and phenylacetylene, respectively, at room temperature.
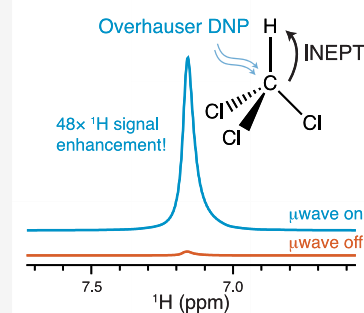
Nuclear magnetic resonance (NMR) spectroscopy is the gold standard for characterizing molecules in solution, with its only real weakness in comparison to other spectroscopic methods being its intrinsically low sensitivity. At room temperature, and the magnetic fields typically used for NMR today (e.g., 9.4 T), the nuclear spin states are polarized to only 0.01%.[1] There is thus intense interest in methods for actively increasing NMR sensitivity. One of the most promising approaches to increasing sensitivity is to transiently increase the polarization of the NMR transitions by so-called hyperpolarization methods, with dynamic nuclear polarization (DNP) being at the forefront of these efforts.[2,3] DNP allows the transfer of the much larger polarization of unpaired electron spins to nuclei.[4] DNP has been very successful in solid-state NMR,[5−10] but its implementation in solution-state NMR has proved much more challenging. Transient hyperpolarized NMR signals can be observed at room temperature using the dissolution DNP approach, where a frozen sample is polarized at 1.2 K followed by rapid dissolution and then shuttling of the solution to an NMR spectrometer.[11] This method provides signal enhancements of 4−5 orders of magnitude on target molecules or bulk solvent molecules with promising applications in magnetic resonance imaging.[12,13] However, the hyperpolarization decays rapidly after dissolution and the technique offers a limited sample throughput.[14] A variety of other approaches to producing transient hyperpolarization such as parahydrogen-induced polarization (PHIP),[15] triplet DNP,[16,17] and relay of optically enhanced polarization via the nuclear Overhauser effect (NOE)[18] have also been proposed.

The Overhauser effect (OE) DNP mechanism is the most promising approach for obtaining steady-state continuous hyperpolarization of nuclei *in situ* and at room temperature.[19−31] Indeed, while the magnetic field dependence of OE is generally unfavorable, it has recently been shown that OE DNP can yield significant ^{13}C or ^{31}P signal enhancements at magnetic fields of ≤14 T.[26,27,29,32−34] For example, Orlando et al. have shown ^{13}C enhancements of ≤600 at 9.4 T for a 35 nL sample in a helix resonator.[27] Dubroca et al. also showed a ^{13}C enhancement[26] of 70 and a ^{31}P enhancement[33] of 160 with sample volumes of 100 μL at 14.1 T, using a custom solution NMR probe and microwave gating to minimize sample heating. In contrast, OE DNP to hyperpolarize ^{1}H in solution at high field is very inefficient.[35] For example, Prisner and co-workers were able to hyperpolarize water with enhancements of −80 at 9.2 T, but only by using microwave superheated temperatures of 160 °C in an ~1 nL sample volume;[36,37] recent improvements in probe design allowed sample volumes of ≤100 nL.[34] There is thus great interest in hyperpolarizing ^{1}H nuclei in solution.

Here we demonstrate a straightforward approach for obtaining ^{1}H DNP enhancements on chloroform, 1,1,2,2-tetrachloroethane (TCE), and phenylacetylene by transferring ^{13}C hyperpolarization generated by OE DNP to the attached ^{1}H spins using the insensitive nuclei enhanced by polarization transfer (INEPT) pulse sequence (Figure 1B).[38] Using a
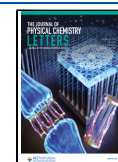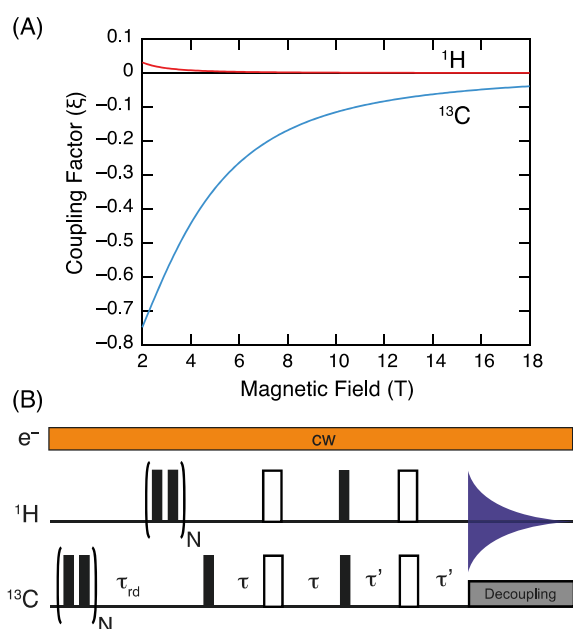
Figure 1. (A) Predicted dependence of the coupling factor (ξ) on the applied magnetic field, calculated as described in the Supporting Information, for ^{1}H (red) and ^{13}C (blue) in chloroform. (B) Pulse sequence used here to obtain ^{1}H hyperpolarization by DNP enhanced ^{13}C → ^{1}H INEPT in the presence of continuous microwave irradiation. N is an integer, and π and π' are delays; further details regarding the pulse sequence are provided in the Supporting Information.

Bruker 9.4 T magic angle spinning (MAS) DNP spectrometer and a commercial solid-state MAS DNP probe, we obtain enhancements of 48, 8, and 6 for chloroform, tetrachloroethane, and phenylacetylene, respectively, at room temperature.

Although ^{13}C NMR is intrinsically less sensitive than ^{1}H NMR, ^{13}C nuclei can in general be much more efficiently hyperpolarized in solution Overhauser DNP experiments. This is primarily due to the large difference in the coupling factors (ξ) between ^{13}C and ^{1}H, as shown in Figure 1A for factors typical for most protons and for carbons such as the ones in chloroform.[24,25] The coupling factor determines enhancement according to the Solomon equation[39]

$$\varepsilon = 1 - \xi f s \frac{\gamma_e}{\gamma_n} \tag{1}$$

where γ_e and γ_n are the gyromagnetic ratios of the electron and the nuclear spin, respectively, f is the leakage factor ($f = 1 - T_{1n}/T_{1n,dia}$, where T_{1n} and $T_{1n,dia}$ are the nuclear T_1 values in the presence and absence of radicals, respectively), s is the saturation factor (described further below), and the coupling factor is determined by the relative weights of the scalar and dipolar hyperfine contributions (as detailed in the Supporting Information). We also see from Figure 1A that the efficiency of OE DNP decreases significantly at higher fields due to the magnetic field dependence of the coupling factors.[24,28,40] Although the pure scalar hyperfine mechanism is independent of field, the contribution of the dipolar mechanism results in a decay of the coupling factor at high fields.[28] Consequently, ^{1}H DNP enhancements, which typically rely on direct dipolar contributions between the unpaired electron and ^{1}H spins, are minimal at high fields.[41]

Here, we suggest that a simple way to obtain ^{1}H enhancements is to transfer the hyperpolarization from ^{13}C to ^{1}H using, for example, a reverse INEPT sequence (Figure 1B)[38,42,43] or cross-polarization[44] in a ^{13}C-enriched substrate. Combining these polarization transfer tools with other approaches to hyperpolarization, including dissolution DNP and PHIP, has been demonstrated.[45−51] Notably, Dey et al. have previously performed ^{1}H→^{13}C transfers to enhance the ^{13}C sensitivity using Overhauser DNP at low fields where ^{1}H

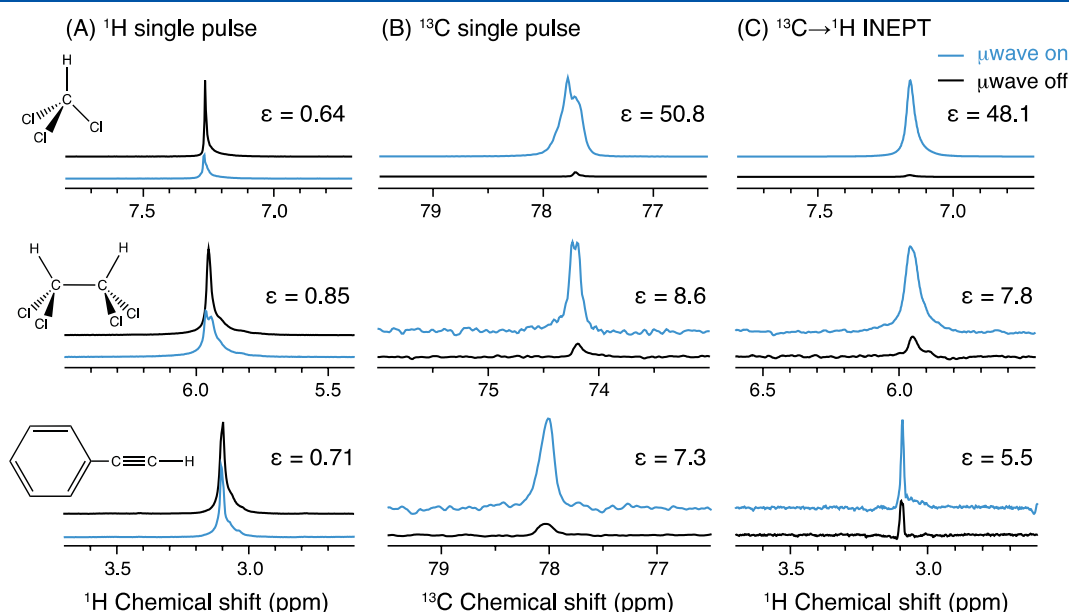**Figure 2.** (A) ^{1}H, (B) ^{13}C, and (C) ^{13}C→^{1}H INEPT NMR spectra obtained at (blue) 9.4 T with and (black) without continuous-wave microwave irradiation using a 263 GHz gyrotron source for (top) [^{13}C$_1$]chloroform, (middle) 1,1,2,2-tetrachloroethane (TCE), and (bottom) phenylacetylene. 10 mM [^{15}N]-d_{16}-TEMPONE (denoted as ^{15}N-TN) radical solutions were used. DNP enhancements (ε) were measured by taking the ratio of the integrated signal intensities of the microwave ON and OFF spectra.
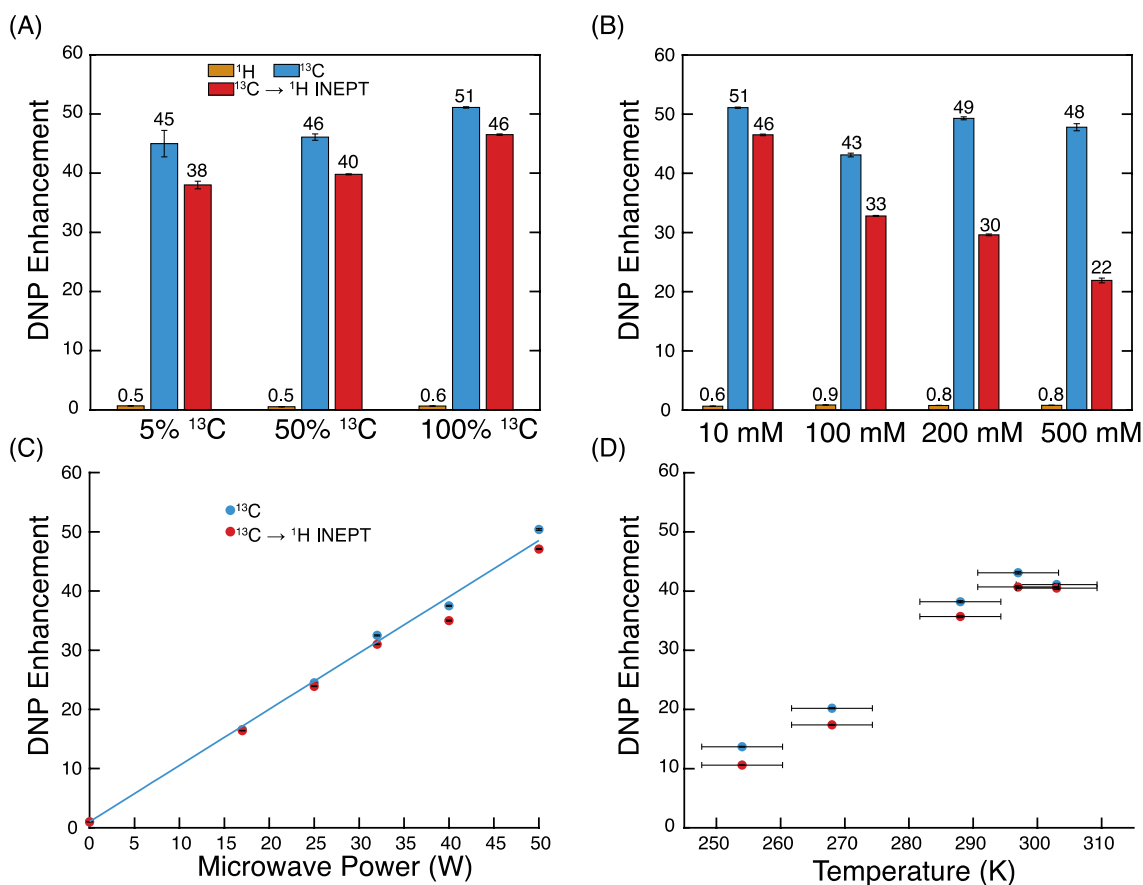
Figure 3. Experimental 9.4 T ^{1}H, ^{13}C, and ^{13}C→^{1}H INEPT DNP enhancements for chloroform with different (A) degrees of ^{13}C labeling and (B) concentrations of ^{15}N-TN. All enhancements were measured with the same absolute temperature maintained for microwave ON and OFF spectra (details in the Supporting Information). DNP enhancement is shown in panel C as a function of applied microwave power (with the fitted straight line in blue) and in panel D as a function of sample temperature for 100% [^{13}C$_1$]chloroform with 10 mM ^{15}N-TN.

hyperpolarization is efficient.[52] INEPT is a well-established method for enhancing the NMR sensitivity of low-gyromagnetic ratio nuclei and/or obtaining through-bond correlation spectra via J couplings.[1] For a fully ^{13}C enriched sample at thermal equilibrium, the ^{1}H magnetization produced by a ^{13}C→^{1}H INEPT experiment will be 25% of that of a directly excited ^{1}H NMR spectrum (in an ideal NMR spectrometer). However, in INEPT experiments under hyperpolarization conditions, the overall sensitivity of the observed nucleus is not only proportional to the ratio of the gyromagnetic ratios of the corresponding nuclei but also determined by the relative hyperpolarization levels. If ^{13}C DNP enhancements of 10−100 can be obtained, neglecting the differences in ^{1}H and ^{13}C T_1 relaxation times, the overall ^{1}H sensitivity could be increased by factors of 2.5−25, corresponding to decreases in experimental times of 1−3 orders of magnitude. At natural abundance, the sensitivity gain in comparison to a one-dimensional (1D) ^{1}H NMR spectrum will of course be reduced by 99% due to the low natural abundance of ^{13}C (NA = 1.1%) as only 1.1% of ^{1}H spins will be hyperpolarized. In addition to abundance, the relaxation rates of the involved nuclei, because they are affected by paramagnetic interactions with the radical polarizing agent (*vide infra*), will affect the INEPT efficiencies, and any differences in efficiency of the two radiofrequency channels in the probe will also impact the sensitivity gains.

Figure 2 shows the direct 1D ^{1}H and ^{13}C Overhauser DNP enhancements obtained for chloroform, TCE, and phenyl-acetylene using 10 mM [^{15}N]-d_{16}-TEMPONE (denoted hereafter as ^{15}N-TN). High-power microwaves (50 W, corresponding to an estimated ν_{1e} of ~1.3 MHz) were applied using a 263 GHz gyrotron microwave source, with 10 μL of the sample placed in 3.2 mm sapphire rotors. While the sapphire rotors that are typical in MAS DNP experiments provide good microwave penetration, the small sample volumes help to minimize temperature gradients. To compensate for the heating caused by microwave irradiation, a low-temperature nitrogen gas flow was applied. With chloroform, we performed experiments using a 100% ^{13}C-labeled solvent. As expected, the direct ^{1}H DNP enhancement was low ($\varepsilon_{^1H}$ = 0.6) due to the poor efficiency of the dipolar Overhauser DNP mechanism. However, a large ^{13}C enhancement ($\varepsilon_{^{13}C}$) of 51 was obtained, which is higher than the enhancement of 17 previously observed at 14.1 T using a similar commercial MAS DNP spectrometer.[27] ^{13}C→^{1}H INEPT experiments were performed using the pulse sequence of Figure 1B to yield a high indirect ^{1}H enhancement ($\varepsilon_{^{13}C→^1H}$) of 48, showing that the enhancement can be transferred from ^{13}C to ^{1}H with >90% efficiency. This corresponds to an overall increase in ^{1}H polarization by a factor 12 (48 × $\gamma_{^{13}C}$/$\gamma_{^1H}$).

To demonstrate the generality of this method, we performed experiments with (natural abundance) samples of TCE and phenylacetylene. With TCE, a direct ^{13}C DNP enhancement of 9 was observed and a corresponding ^{13}C→^{1}H INEPT enhancement of 8 was obtained. Note that the enhancement

decreases from chloroform to TCE likely due to weaker electron–nuclear scalar hyperfine couplings resulting in a coupling factor that is 16% of that of chloroform, assuming the same saturation and leakage factors. Phenylacetylene has a terminal alkyne carbon that interacts with nitroxide radicals and has been shown to display reasonable enhancements.[24,26] With our protocol, we observed a ^{13}C enhancement of 7 and an INEPT enhancement of 5 on the alkyne CH group, which are larger than the enhancements for the other carbons in the molecule, in good agreement with the literature (Figure S1).[24,26]

The frequency of collision between radicals and the target species has been shown to be important to the OE DNP mechanism.[29,41] We studied the enhancements as a function of the degree of ^{13}C labeling and radical concentration to obtain optimal DNP enhancements (Figure 3). As the results shown in panels A and B of Figure 3 illustrate, neither the degree of ^{13}C labeling nor the radical concentration affects the direct ^{13}C DNP enhancement of chloroform by >15%. The ^{13}C DNP enhancement is not expected to change with the degree of ^{13}C labeling because the frequency of collision per ^{13}C remains unchanged. Note that the ^{13}C enhancement obtained for chloroform here is larger than that of the terminal carbon of phenylacetylene by a factor of 7, while a factor of 2 was observed in a previous study at 14.1 T using ^{13}C-labeled samples; however, these experiments were performed in dilute solutions.[26] On the contrary, we expected the enhancements to be dependent on radical concentration as demonstrated previously;[27,36] the absence of a significant change in ^{13}C DNP enhancement (Figure 3B) suggests that changes in the coupling and the saturation factors likely cancel each other here.

DNP enhancements measured at different microwave powers verified that the optimal condition is at the maximum microwave power attainable with our system because both ^{13}C and INEPT enhancements increase almost linearly with microwave power (Figure 3C). By using eq 1 and the coupling factor from the literature,[27] we back-calculated the saturation factor at 50 W to be 0.115 (see section S3.1 of the Supporting Information), which supports that the enhancement is saturation-limited. Consistent with our observation, the saturation factor of eq 2a[53] for two coupled hyperfine transitions shows a linear relationship with B_1^2, which is proportional to the microwave power, when $\gamma_e^2 B_1^2 T_{1e} T_{2e} \ll 1$ as shown in eq 2b.

$$\frac{1}{s} = \frac{2(2w_{1e} + w_{1n}) + \omega_{ex}}{2(w_{1e} + w_{1n}) + \omega_{ex}} + \frac{2}{\gamma_e^2 B_1^2 T_{1e} T_{2e}} \tag{2a}$$

where w_{1e}, w_{1n}, and ω_{ex} are the electron spin–lattice relaxation rate $[w_{1e} = 1/(2T_{1e})]$, the nuclear spin relaxation rate ($w_{1n} = 1/T_{1n}$), and the Heisenberg spin exchange rate, respectively, and where we find

$$s = \frac{1}{2}\gamma_e^2 B_1^2 T_{1e} T_{2e} \tag{2b}$$

when $\gamma_e^2 B_1^2 T_{1e} T_{2e} \ll 1$. Furthermore, from eq 2a, we estimate that the corresponding B_1 field in the sample is approximately 0.05 mT ($\nu_1 = 1.3$ MHz) by using $T_{1e} T_{2e} = 3.5 \times 10^{-15}$ s^2 from the literature[54] (see section S3.1). In comparison, a microwave field of 0.16 mT was obtained previously with 30 W of power on a specialized liquid-state Overhauser DNP probe.[26]

Upon microwave irradiation, significant peak broadening was observed, which can be attributed to a temperature gradient across the sample as we meanwhile observed T_2 changes within the peak (see Figure S3). To further examine the impact of sample temperature, we carried out a series of experiments with and without microwave irradiation at different temperatures by actively adjusting the temperature of the cooling gas (Tables S8 and S9). To avoid boiling the chloroform, we tested the behavior below ambient temperature. The measured temperature dependence of the enhancement depicted in Figure 3D clearly shows decreasing DNP performance with lower temperatures. When the temperature was decreased from 300 to 255 K, an 80% reduction in enhancement was observed. This trend has been observed with CCl$_4$ and can be explained by a less negative coupling factor at low temperature as suggested by theoretical studies.[25,27]

The performance of the INEPT scheme is impacted if there is significant relaxation during the τ and τ' delays. The INEPT efficiency is related to the measured relaxation times according to

$$I_{INEPT} = \sin(2\pi\tau J) \times \sin(2\pi\tau' J) \times e^{-2\tau\left(\frac{1}{T_{1,H}} + \frac{1}{T_{2,C}}\right) - 2\tau'\left(\frac{1}{T_{1,C}} + \frac{1}{T_{2,H}}\right)} \tag{3}$$

During the τ and τ' delays of the INEPT sequence, the antiphase coherences leading to the INEPT signal will decay with the relaxation times of both ^{1}H and ^{13}C.[1] (Because the $^1J_{CH}$ coupling constant in chloroform is 210 Hz, both τ and τ' were therefore set to $1/4J_{CH}$, 1.19 ms.) For the samples with a radical concentration of 10 mM, the nuclear relaxation times are longer than τ by at least 1 order of magnitude as Figure 4A shows, which means that the magnetization of ^{13}C can be successfully transferred to ^{1}H, with INEPT efficiencies of >90% as shown in Figure 4B. However, when the radical concentration is increased from 10 to >100 mM, the efficiency of INEPT transfer decreases significantly, to ~25% at 500 mM (Figure 4B).

Because the absolute transfer efficiency is dependent on relaxation, the differences in nuclear relaxation times between microwave ON and OFF experiments due to the temperature gradient will make the DNP enhancement measured by INEPT deviate from the direct ^{13}C enhancement (Figure S2). Among our experiments using chloroform, we consistently observed shorter overall nuclear T_2 values under microwave irradiation (Table S5). Consequently, the INEPT efficiency with microwave irradiation is lower than the corresponding efficiency without microwaves, which reduces the INEPT DNP enhancement. However, this effect is negligible when nuclear relaxation times are significantly longer than τ, which is the case at a low radical concentration as we show in Figure 4B when the radical concentration is 10 mM. When these two effects are combined, the high radical concentration is not favorable for INEPT due to the low absolute INEPT efficiency and the sensitivity of INEPT efficiency to relaxation time fluctuation.

In conclusion, we have demonstrated a simple method for obtaining bulk ^{1}H hyperpolarization in solution by efficiently transferring ^{13}C hyperpolarization generated by the Overhauser effect to ^{1}H with a reverse INEPT pulse sequence. Here, this method yields an overall increase in ^{1}H polarization of a factor 12 for a bulk solution of $[^{13}C_1]$chloroform and is limited by the constraints of our experimental setup. This should be a generally applicable method for hyperpolarizing ^{1}H nuclei that
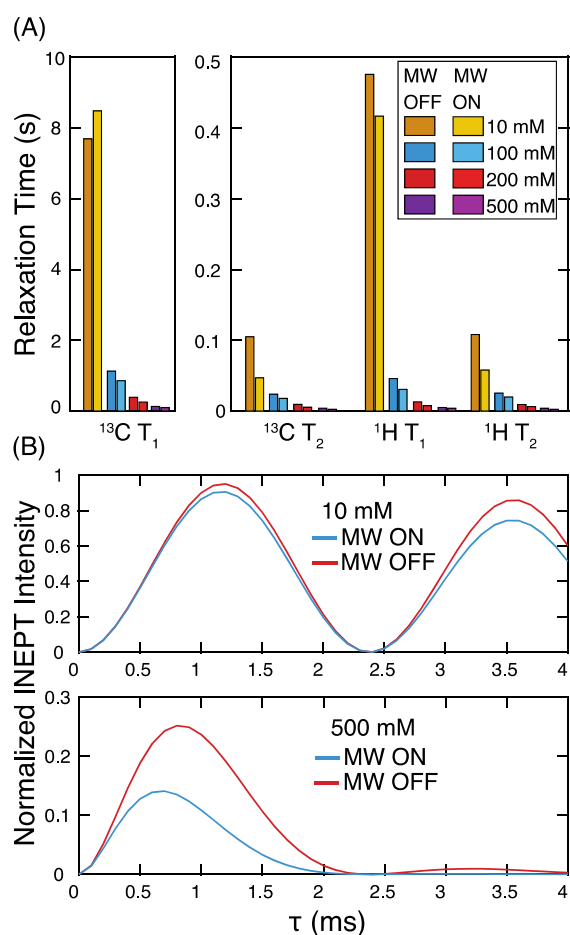
Figure 4. (A) Plot showing the variation of measured nuclear spin relaxation times with radical concentration at room temperature with and without microwave irradiation. (B) Plot showing the normalized INEPT signal intensity as a function of the length of the τ delay in the reverse INEPT pulse sequence shown in Figure 1B. Only radical concentrations of 10 and 500 mM are shown; others are shown in Figure S2.

otherwise give intrinsically poor OE DNP enhancement at high magnetic fields. The approach demonstrated here could also be potentially extended to sources containing other abundant heteronuclei such as ^{31}P.

■ ASSOCIATED CONTENT

ⓈⒾ Supporting Information

The Supporting Information is available free of charge at https://pubs.acs.org/doi/10.1021/acs.jpclett.2c01956.

Additional figures, tables, and experimental details and a link to all of the raw NMR data (PDF)

■ AUTHOR INFORMATION

Corresponding Author

Lyndon Emsley − *Institut des Sciences et Ingénierie Chimiques, Ecole Polytechnique Fédérale de Lausanne (EPFL), CH-1015 Lausanne, Switzerland;* ⓞ orcid.org/0000-0003-1360-2572; Email: lyndon.emsley@epfl.ch

Authors

Yu Rao − *Institut des Sciences et Ingénierie Chimiques, Ecole Polytechnique Fédérale de Lausanne (EPFL), CH-1015 Lausanne, Switzerland;* ⓞ orcid.org/0000-0002-9787-5596

Amrit Venkatesh − *Institut des Sciences et Ingénierie Chimiques, Ecole Polytechnique Fédérale de Lausanne (EPFL), CH-1015 Lausanne, Switzerland;* ⓞ orcid.org/0000-0001-5319-9269

Pinelopi Moutzouri − *Institut des Sciences et Ingénierie Chimiques, Ecole Polytechnique Fédérale de Lausanne (EPFL), CH-1015 Lausanne, Switzerland*

Complete contact information is available at:
https://pubs.acs.org/10.1021/acs.jpclett.2c01956

Notes

The authors declare no competing financial interest.

■ REFERENCES

(1) Keeler, J. *Understanding NMR spectroscopy*; John Wiley & Sons, 2011.

(2) Ardenkjaer-Larsen, J. H.; Boebinger, G. S.; Comment, A.; Duckett, S.; Edison, A. S.; Engelke, F.; Griesinger, C.; Griffin, R. G.; Hilty, C.; Maeda, H.; Parigi, G.; Prisner, T.; Ravera, E.; van Bentum, J.; Vega, S.; Webb, A.; Luchinat, C.; Schwalbe, H.; Frydman, L. Facing and overcoming sensitivity challenges in biomolecular NMR spectroscopy. *Angew. Chem., Int. Ed.* **2015**, *54*, 9162−9185.

(3) Jeschke, G.; Frydman, L. Nuclear hyperpolarization comes of age. *J. Magn. Reson.* **2016**, *264*, 1−2.

(4) Abragam, A. *The principles of nuclear magnetism*; Oxford University Press, 1961.

(5) Maly, T.; Debelouchina, G. T.; Bajaj, V. S.; Hu, K. N.; Joo, C. G.; Mak-Jurkauskas, M. L.; Sirigiri, J. R.; van der Wel, P. C. A.; Herzfeld, J.; Temkin, R. J.; Griffin, R. G. Dynamic nuclear polarization at high magnetic fields. *J. Chem. Phys.* **2008**, *128*, 052211.

(6) Lesage, A.; Lelli, M.; Gajan, D.; Caporini, M. A.; Vitzthum, V.; Mieville, P.; Alauzun, J.; Roussey, A.; Thieuleux, C.; Mehdi, A.; Bodenhausen, G.; Coperet, C.; Emsley, L. Surface enhanced NMR spectroscopy by dynamic nuclear polarization. *J. Am. Chem. Soc.* **2010**, *132*, 15459−15461.

(7) Rossini, A. J.; Zagdoun, A.; Lelli, M.; Lesage, A.; Coperet, C.; Emsley, L. Dynamic nuclear polarization surface enhanced NMR spectroscopy. *Acc. Chem. Res.* **2013**, *46*, 1942−1951.

(8) Ni, Q. Z.; Daviso, E.; Can, T. V.; Markhasin, E.; Jawla, S. K.; Swager, T. M.; Temkin, R. J.; Herzfeld, J.; Griffin, R. G. High frequency dynamic nuclear polarization. *Acc. Chem. Res.* **2013**, *46*, 1933−1941.

(9) Lilly Thankamony, A. S.; Wittmann, J. J.; Kaushik, M.; Corzilius, B. Dynamic nuclear polarization for sensitivity enhancement in modern solid-state NMR. *Prog. Nucl. Magn. Reson. Spectrosc.* **2017**, *102−103*, 120−195.

(10) Reif, B.; Ashbrook, S. E.; Emsley, L.; Hong, M. Solid-state NMR spectroscopy. *Nat. Rev. Methods Primers* **2021**, *1*, 4.

(11) Ardenkjaer-Larsen, J. H.; Fridlund, B.; Gram, A.; Hansson, G.; Hansson, L.; Lerche, M. H.; Servin, R.; Thaning, M.; Golman, K. Increase in signal-to-noise ratio of > 10,000 times in liquid-state NMR. *Proc. Natl. Acad. Sci. U.S.A.* **2003**, *100*, 10158−10163.

(12) Ardenkjaer-Larsen, J. H. On the present and future of dissolution-DNP. *J. Magn. Reson.* **2016**, *264*, 3−12.

(13) Hilty, C.; Kurzbach, D.; Frydman, L. Hyperpolarized water as universal sensitivity booster in biomolecular NMR. *Nat. Protoc.* **2022**, *17*, 1621−1657.

(14) Jannin, S.; Dumez, J. N.; Giraudeau, P.; Kurzbach, D. Application and methodology of dissolution dynamic nuclear polarization in physical, chemical and biological contexts. *J. Magn. Reson.* **2019**, *305*, 41−50.

(15) Duckett, S. B.; Mewis, R. E. Application of parahydrogen induced polarization techniques in NMR spectroscopy and imaging. *Acc. Chem. Res.* **2012**, *45*, 1247−1257.

(16) Dale, M. W.; Wedge, C. J. Optically generated hyperpolarization for sensitivity enhancement in solution-state NMR spectroscopy. *Chem. Commun.* **2016**, *52*, 13221−13224.

(17) Liu, G. Q.; Liou, S. H.; Enkin, N.; Tkach, I; Bennati, M. Photoinduced radical polarization and liquid-state dynamic nuclear polarization using fullerene nitroxide derivatives. *Phys. Chem. Chem. Phys.* **2017**, *19*, 31823−31829.

(18) Eichhorn, T. R.; Parker, A. J.; Josten, F.; Muller, C.; Scheuer, J.; Steiner, J. M.; Gierse, M.; Handwerker, J.; Keim, M.; Lucas, S.; Qureshi, M. U.; Marshall, A.; Salhov, A.; Quan, Y. F.; Binder, J.; Jahnke, K. D.; Neumann, P.; Knecht, S.; Blanchard, J. W.; Plenio, M. B.; Jelezko, F.; Emsley, L.; Vassiliou, C. C.; Hautle, P.; Schwartz, I. Hyperpolarized solution-state NMR spectroscopy with optically polarized crystals. *J. Am. Chem. Soc.* **2022**, *144*, 2511−2519.

(19) Hausser, K. H.; Stehlik, D. Dynamic nuclear polarization in liquids. In *Advances in Magnetic and Optical Resonance*; Waugh, J. S., Ed.; Advances in Magnetic Resonance, Vol. 3; Academic Press, 1968; pp 79−139.

(20) Mullerwarmuth, W.; Meisegresch, K. Molecular motions and interactions as studied by dynamic nuclear polarization (DNP) in free radical solutions. *Adv. Magn. Reson.* **1983**, *11*, 1−45.

(21) Loening, N. M.; Rosay, M.; Weis, V.; Griffin, R. G. Solution-state dynamic nuclear polarization at high magnetic field. *J. Am. Chem. Soc.* **2002**, *124*, 8808−8809.

(22) Hofer, P.; Parigi, G.; Luchinat, C.; Carl, P.; Guthausen, G.; Reese, M.; Carlomagno, T.; Griesinger, C.; Bennati, M. Field dependent dynamic nuclear polarization with radicals in aqueous solution. *J. Am. Chem. Soc.* **2008**, *130*, 3254−3255.

(23) Denysenkov, V.; Prandolini, M. J.; Gafurov, M.; Sezer, D.; Endeward, B.; Prisner, T. F. Liquid state DNP using a 260 GHz high power gyrotron. *Phys. Chem. Chem. Phys.* **2010**, *12*, 5786−5790.

(24) Wang, X.; Isley, W. C., III; Salido, S. I.; Sun, Z.; Song, L.; Tsai, K. H.; Cramer, C. J.; Dorn, H. C. Optimization and prediction of the electron-nuclear dipolar and scalar interaction in ^{1}H and ^{13}C liquid state dynamic nuclear polarization. *Chem. Sci.* **2015**, *6*, 6482−6495.

(25) Liu, G.; Levien, M.; Karschin, N.; Parigi, G.; Luchinat, C.; Bennati, M. One-thousand-fold enhancement of high field liquid nuclear magnetic resonance signals at room temperature. *Nat. Chem.* **2017**, *9*, 676−680.

(26) Dubroca, T.; Wi, S.; van Tol, J.; Frydman, L.; Hill, S. Large volume liquid state scalar Overhauser dynamic nuclear polarization at high magnetic field. *Phys. Chem. Chem. Phys.* **2019**, *21*, 21200−21204.

(27) Orlando, T.; Dervişoğlu, R.; Levien, M.; Tkach, I.; Prisner, T. F.; Andreas, L. B.; Denysenkov, V. P.; Bennati, M. Dynamic nuclear polarization of ^{13}C nuclei in the liquid state over a 10 T field range. *Angew. Chem., Int. Ed.* **2019**, *58*, 1402−1406.

(28) Bennati, M.; Orlando, T. Overhauser DNP in Liquids on ^{13}C Nuclei. *eMagRes* **2019**, *8*, 11−18.

(29) Levien, M.; Hiller, M.; Tkach, I.; Bennati, M.; Orlando, T. Nitroxide derivatives for dynamic nuclear polarization in liquids: the role of rotational diffusion. *J. Phys. Chem. Lett.* **2020**, *11*, 1629−1635.

(30) Levien, M.; Reinhard, M.; Hiller, M.; Tkach, I.; Bennati, M.; Orlando, T. Spin density localization and accessibility of organic radicals affect liquid-state DNP efficiency. *Phys. Chem. Chem. Phys.* **2021**, *23*, 4480−4485.

(31) Jakdetchai, O.; Denysenkov, V.; Becker-Baldus, J.; Dutagaci, B.; Prisner, T. F.; Glaubitz, C. Dynamic nuclear polarization-enhanced NMR on aligned lipid bilayers at ambient temperature. *J. Am. Chem. Soc.* **2014**, *136*, 15533−15536.

(32) Yoon, D.; Dimitriadis, A. I.; Soundararajan, M.; Caspers, C.; Genoud, J.; Alberti, S.; de Rijk, E.; Ansermet, J. P. High-field liquid-state dynamic nuclear polarization in microliter samples. *Anal. Chem.* **2018**, *90*, 5620−5626.

(33) Dubroca, T.; Smith, A. N.; Pike, K. J.; Froud, S.; Wylde, R.; Trociewitz, B.; Mckay, J.; Mentink-Vigier, F.; van Tol, J.; Wi, S.; Brey, W.; Long, J. R.; Frydman, L.; Hill, S. A quasi-optical and corrugated waveguide microwave transmission system for simultaneous dynamic nuclear polarization NMR on two separate 14.1 T spectrometers. *J. Magn. Reson.* **2018**, *289*, 35−44.

(34) Dai, D. H.; Wang, X. W.; Liu, Y. W.; Yang, X. L.; Glaubitz, C.; Denysenkov, V.; He, X.; Prisner, T.; Mao, J. F. Room-temperature dynamic nuclear polarization enhanced NMR spectroscopy of small biological molecules in water. *Nat. Commun.* **2021**, *12*, 6880.

(35) Denysenkov, V. P.; Prisner, T. F. Liquid-state Overhauser DNP at high magnetic fields. *eMagRes* **2019**, *8*, 41−54.

(36) Neugebauer, P.; Krummenacker, J. G.; Denysenkov, V. P.; Parigi, G.; Luchinat, C.; Prisner, T. F. Liquid state DNP of water at 9.2 T: an experimental access to saturation. *Phys. Chem. Chem. Phys.* **2013**, *15*, 6049−6056.

(37) Prisner, T.; Denysenkov, V.; Sezer, D. Liquid state DNP at high magnetic fields: Instrumentation, experimental results and atomistic modelling by molecular dynamics simulations. *J. Magn. Reson.* **2016**, *264*, 68−77.

(38) Morris, G. A.; Freeman, R. Enhancement of nuclear magnetic-resonance signals by polarization transfer. *J. Am. Chem. Soc.* **1979**, *101*, 760−762.

(39) Solomon, I. Relaxation processes in a system of two spins. *Phys. Rev.* **1955**, *99*, 559−565.

(40) Bennati, M.; Luchinat, C.; Parigi, G.; Turke, M. T. Water ^{1}H relaxation dispersion analysis on a nitroxide radical provides information on the maximal signal enhancement in Overhauser dynamic nuclear polarization experiments. *Phys. Chem. Chem. Phys.* **2010**, *12*, 5902−5910.

(41) Orlando, T.; Kuprov, I.; Hiller, M. Theoretical analysis of scalar relaxation in ^{13}C-DNP in liquids. *J. Magn. Reson. Open* **2022**, *10*, 100040.

(42) Burum, D. P.; Ernst, R. R. Net polarization transfer via a J-ordered state for signal enhancement of low-sensitivity nuclei. *J. Magn. Reson.* **1980**, *39*, 163−168.

(43) Bax, A.; Freeman, R.; Morris, G. Correlation of proton chemical-shifts by two-dimensional fourier-transform NMR. *J. Magn. Reson.* **1981**, *42*, 164−168.

(44) Pines, A.; Gibby, M. G.; Waugh, J. S. Proton-enhanced NMR of dilute spins in solids. *J. Chem. Phys.* **1973**, *59*, 569−590.

(45) Chekmenev, E. Y.; Norton, V. A.; Weitekamp, D. P.; Bhattacharya, P. Hyperpolarized ^{1}H NMR employing low gamma nucleus for spin polarization storage. *J. Am. Chem. Soc.* **2009**, *131*, 3164−3165.

(46) Giraudeau, P.; Shrot, Y.; Frydman, L. Multiple ultrafast, broadband 2D NMR spectra of hyperpolarized natural products. *J. Am. Chem. Soc.* **2009**, *131*, 13902−13903.

(47) Sarkar, R.; Comment, A.; Vasos, P. R.; Jannin, S.; Gruetter, R.; Bodenhausen, G.; Hall, H.; Kirik, D.; Denisov, V. P. Proton NMR of ^{15}N-Choline metabolites enhanced by dynamic nuclear polarization. *J. Am. Chem. Soc.* **2009**, *131*, 16014−16015.

(48) Vasos, P. R.; Comment, A.; Sarkar, R.; Ahuja, P.; Jannin, S.; Ansermet, J. P.; Konter, J. A.; Hautle, P.; van den Brandt, B.; Bodenhausen, G. Long-lived states to sustain hyperpolarized magnetization. *Proc. Natl. Acad. Sci. U.S.A.* **2009**, *106*, 18469−18473.

(49) Dzien, P.; Fages, A.; Jona, G.; Brindle, K. M.; Schwaiger, M.; Frydman, L. Following metabolism in living microorganisms by hyperpolarized ^{1}H NMR. *J. Am. Chem. Soc.* **2016**, *138*, 12278−12286.

(50) Wang, J. Z.; Kreis, F.; Wright, A. J.; Hesketh, R. L.; Levitt, M. H.; Brindle, K. M. Dynamic ^{1}H imaging of hyperpolarized [1-^{13}C]lactate in vivo using a reverse INEPT experiment. *Magn. Reson. Med.* **2018**, *79*, 741−747.

(51) Bielytskyi, P.; Grasing, D.; Mote, K. R.; Sai Sankar Gupta, K. B.; Vega, S.; Madhu, P. K.; Alia, A.; Matysik, J. ^{13}C -> ^{1}H transfer of light-induced hyperpolarization allows for selective detection of protons in

frozen photosynthetic reaction center. *J. Magn. Reson.* **2018**, *293*, 82−91.

(52) Dey, A.; Banerjee, A.; Chandrakumar, N. Transferred Overhauser DNP: a fast, efficient approach for room temperature ^{13}C ODNP at moderately low fields and natural abundance. *J. Phys. Chem. B* **2017**, *121*, 7156−7162.

(53) Turke, M. T.; Parigi, G.; Luchinat, C.; Bennati, M. Overhauser DNP with ^{15}N labelled Fremy's salt at 0.35 T. *Phys. Chem. Chem. Phys.* **2012**, *14*, 502−510.

(54) Denysenkov, V. P.; Prandolini, M. J.; Krahn, A.; Gafurov, M.; Endeward, B.; Prisner, T. F. High-field DNP spectrometer for liquids. *Appl. Magn. Reson.* **2008**, *34*, 289−299.